Published in final edited form as:
J Orthop Res. 2010 August ; 28(8): 992–999. doi:10.1002/jor.21115.

Cefazolin Embedded Biodegradable Polypeptide Nanofilms Promising for Infection Prevention: A Preliminary Study on Cell Responses

Hongshuai Li, MD, PhD[1], **Heather Ogle, BS**[1], **Bingbing Jiang, PhD**[1], **Michael Hagar, BS**[1], and **Bingyun Li, PhD**[1,2,3,*]

[1]Department of Orthopaedics, School of Medicine, West Virginia University, Morgantown, WV 26506, USA

[2]WVNano Initiative, Morgantown, WV 26506, USA

[3]Department of Chemical Engineering, College of Engineering and Mineral Resources, West Virginia University, Morgantown, WV 26506, USA

Abstract

Implant-associated infection is a serious complication in orthopedic surgery, and endowing implant surfaces with antibacterial properties could be one of the most promising approaches for preventing such infection. In this study, we developed cefazolin loaded biodegradable polypeptide multilayer nanofilms on orthopedic implants. We found that the amount of cefazolin released could be tuned. A high local concentration of cefazolin was achieved within the first a few hours and therefore may inhibit bacterial colonization in the critical post-implantation period. The developed cefazolin loaded nanofilms showed their *in vitro* efficacy against *Staphylococcus aureus* (*S. aureus*); the more antibiotics loaded, the longer the nanocoated implant had antibacterial properties. More interestingly, antibiotic-loaded polypeptide multilayer nanofilms also improved osteoblast bioactivity including cell viability and proliferation. These findings suggested that biodegradable polypeptide multilayer nanofilms as antibiotic carriers at the implant/tissue interface are compatible with human cells such as osteoblasts and bactericidal to bacteria such as *S. aureus*. These characteristics could be promising for preventing implant-associated infection and potentially improving bone healing.

Keywords

Implant-associated infection; local antibiotic delivery; electrostatic layer-by-layer self-assembly; antibiotic; polypeptide

INTRODUCTION

Implant-associated infection is one of the most serious complications in orthopedic surgery. Of the more than two million orthopedic implants used in patients annually in the United States, approximately 4% get infected[1]. The number of implant-associated infections will continue to rise as more baby boomers receive biomedical implants. Bone infections associated with foreign body materials are especially difficult to treat. Removal of the infected implants[2,3], long-term systemic antibiotic therapy, and multiple revisions with

[*]*Correspondence to:* Bingyun Li, PhD, Director, Biomaterials, Bioengineering & Nanotechnology Laboratory, Department of Orthopaedics, School of Medicine, West Virginia University, Morgantown, WV 26506-9196, USA, Tel: 1-304-293-1075, Fax: 1-304-293-7070, bli@hsc.wvu.edu, URL: http://www.hsc.wvu.edu/som/ortho/nanomedica-group/.

radical debridement are frequently required[1,4,5]. The consequences of infection can be devastating and may lead to prolonged hospitalization, poor functional outcome, sepsis, and even amputation[6].

The most probable reason that implant-associated infection is difficult to treat is that pathogens, primarily *S. aureus* and *S. epidermidis*, colonize on the implant surface and form a bio-film[7–10]. Bio-films are resistant to both the immune response and systemic antibiotic therapies[1]. It is, therefore, of great importance to prevent the initial bacterial adhesion thereby preventing bio-film formation on implants. Antibiotic coatings on implants could be an effective approach to reduce bacterial colonization *in vitro* and bio-film formation *in vivo*[11–13].

Many approaches for surface coating, such as dip coating, spin coating, and plasma spray, have been developed to achieve an antibacterial surface[14–16]. Among these techniques, electrostatic layer-by-layer (LBL) self-assembly nanotechnology is one of the most promising methods[17]. This method is simply based on the alternative deposition of oppositely charged polyelectrolyte layers. The driving force for film construction is the alternating charges (positive and negative) that appear after each layer of polyelectrolyte deposition. This technique offers multiple advantages over other approaches. First, the buildup process may be easily performed by simple adsorption procedures on any surfaces of devices used in clinical applications. Second, the formed films may possibly be used as carriers of proteins and other biologically active molecules that can be incorporated without losing their bioactivity[18–20]. Using this technique, a biodegradable coating may be developed to deliver ideal drug dosages over a desirable time period leaving no residual materials on implants[21,22].

The objectives of this study were: (i) to develop biodegradable polypeptide multilayer nanofilms potentially serving as antibiotic carriers at the implant/tissue interface; (ii) to evaluate the efficacy of cefazolin loaded poly(L-lysine)/poly(L-glutamic acid) (PLL/PLGA) nanofilms on stainless steel disks (SSDs), in killing *S. aureus*; and (iii) to evaluate the effects of cefazolin loaded nanofilms on osteoblast cell behavior.

MATERIALS AND METHODS

Layer-by-layer Nanocoating and Cefazolin Loading and Release

SSDs of 10 mm in diameter and 0.25 mm thick were thoroughly cleaned and polypeptide multilayer nanofilms were developed using the LBL technique. Details of the LBL process were reported earlier[23]. The thickness, measured by ellipsometry[24], of 40 layers of PLL and PLGA or PLL/$PLGA_{20}$ nanofilms was about 240 nm.

PLL/$PLGA_{20}$ nanofilms were loaded with cefazolin by immersing them in a cefazolin solution (pH 7) of 2.5, 5, and 10 mg/ml for 20 min. In the *in vitro* release studies, cefazolin-loaded PLL/$PLGA_{20}$ nanocoated SSDs were incubated in 10 ml phosphate buffered saline or PBS (pH 7) at 37°C. 0.6 ml of PBS aliquot solution was taken to determine cefazolin concentration at predetermined time points and 0.6 ml fresh PBS was added afterward.

In vitro Bacterial Inhibition Study

Therapeutic activities of PLL/$PLGA_{20}$ nanofilms were assessed against proliferation of *S. aureus*, which was isolated from a patient with chronic osteomyelitis. A freshly cultured *S. aureus* suspension was centrifuged, then washed and diluted with PBS to contain ~1×10^8 colony forming units (CFU)/ml. The suspension was used for two types of bacterial inhibition assays (see Supplementary Materials): zone of inhibition (ZOI) test and a modified bacterial killing assay[25].

In vitro Bacterial Adhesion Study

A *S. aureus* suspension, containing ~1×10^7 CFU/ml of *S. aureus* was prepared. A highly lipophilic carocyanine dye, i.e. Dio, was used to stain *S. aureus* before seeding onto SSDs. A 1 ml *S. aureus* suspension was then added to a 24-well plate containing bare SSDs or PLL/$PLGA_{20}$ nanocoated SSDs (without cefazolin) and cultured at 37°C for 2 h. After washing with PBS three times and fixing using 10% formalin, the SSDs were glued onto glass slides and observed under confocal fluorescent microscopy (LSM 700, Carl Zeiss, Germany) with excitation/emission wavelengths of 480 nm/505 nm.

Osteoblast Cell Adhesion and Visualization

CRL-11372 human osteoblast cell line (American Type Culture Collection or ATCC, Manassas, VA) was routinely grown In Dulbecco's Modified Eagle's Medium/Ham's Nutrient Mixture F-12, 1:1 medium (DMEM: F-12 medium, ATCC) with 10% fetal bovine serum (ATCC), 100 I.U./ml penicillin, and 100 μg/ml streptomycin (ATCC) in a 5% CO_2 and 95% air atmosphere incubator at 37°C. Cells were also cultured in the absence of penicillin and streptomycin, and used to study osteoblast adhesion and viability (See Supplementary Materials). Cells were seeded on SSD samples in a 24-well plate at 1×10^5 cells/well and incubated at 37°C in a 5% CO_2 humidified incubator. After culturing for 2 and 24 h, the number of adherent cells were examined using hemocytometry. The SSDs were rinsed three times with PBS and transferred to a new 24-well plate. The cells on the SSD samples were then detached with 0.25% Trypsin/0.53 mM EDTA solution (ATCC) followed by rinsing with culture medium. The rinsing media was collected and the number of detached cells was determined using a hemocytometer.

The distribution and morphology of osteoblasts adhered on the SSDs were examined using scanning electron microscopy (SEM) and confocal fluorescent microscopy. After culturing for 2 and 24 h, the cell-seeded SSDs were rinsed with PBS, fixed in 2.5% glutaraldehyde, and post-fixed in 4% osmium tetroxide. The fixed specimens were dehydrated by immersing them into increasing concentrations of ethanol (70%, 85%, 95% and 100%). Then all specimens were dried using a critical point dryer (CPD030, Bal-Tec, Carlsbad, CA). The specimens were observed under SEM (S-4700, Hitachi, Japan). For confocal fluorescent microscopy, cells were stained with a highly lipophilic carocyanine dye Dil before seeding onto the SSDs. Nanocoated and bare SSDs were incubated with the labeled cells for 2 and 24 h. The adherent osteoblasts were observed under confocal fluorescent microscopy with excitation/emission wavelengths of 540 nm/560 nm.

Cell Viability

Cell viability was determined by MTT assay using an *in vitro* toxicology kit (Sigma-Aldrich, St. Louis, MO). Osteoblasts were seeded on SSDs, incubated at 37°C for 4 days, and 200 μl of MTT solution was added to each well and incubated for 2 h. Then, 200 μl of MTT solubilization solution was added to each well and the dissolved solution was transferred to a 96-well plate. Absorbance at 570 nm was measured using a micro-plate reader (μQuant, Bio-Tek, Winooski, VT). The background absorbances of multiwell plates were measured at 690 nm and subtracted from the 570 nm measurements.

Cell Proliferation

Cells were seeded on SSDs at a density of 2×10^5 cells/well. Sample solutions were collected on days 1, 3, and 5. Briefly, osteoblasts adhered to the surface of SSDs were gently rinsed with PBS, overlaid with 1 ml Trypsin/EDTA solution per well and incubated at 37°C for 5 min. The loosely detached cell layer was then scraped off the SSD substrate, centrifuged at 1,200 rpm for 7 min, and re-suspended in 1 ml distilled water with 1% Triton X-100. Then

the cell suspensions underwent three freeze-thaw cycles. The triton lysates were stored at −80°C until testing for DNA content. A 30 μl aliquot of cell suspension was used to determine dsDNA content, which was measured by a fluorometric quantification method using a Quant-iT dsDNA high-sensitivity assay kit (Invitrogen, Carlsbad, CA).

Statistical Methods

Data were expressed as the mean ± standard deviation (SD). Statistical differences were analyzed using the *one-way* ANOVA analysis. $p<0.05$ was considered statistically significant. SPSS software 11.0 was used for statistical analysis.

RESULTS

Cefazolin Release from Polypeptide Nanofilms

Different amounts of cefazolin were loaded into PLL/$PLGA_{20}$ nanofilms; all the nanofilms had similar pharmacokinetics (Fig. 1). All nanofilms had a burst release of cefazolin in the first 2 h followed by a release of 16% or less afterwards. The PLL/$PLGA_{20}$ nanofilms loaded with cefazolin at a higher antibiotic concentration contained a higher amount of antibiotic and subsequently eluted more antibiotics. The PLL/$PLGA_{20}$ nanofilms on SSDs loaded in 2.5, 5.0, and 10.0 mg/ml cefazolin solutions released 64 (84% of total), 125 (91% of total), and 147 μg/cm^2 (93% of total), respectively, of cefazolin at 2 h, and increased to 76, 136, and 157 μg/cm^2, respectively, at the end of the time period studied (i.e. 7 days). In addition, under the same conditions, much more cefazolin was released from PLL/$PLGA_{20}$ nanofilms on quartz slides (~250 μg/cm^2)[24] than on SSDs (~150 μg/cm^2) as the surface properties vary.

In Vitro Antibacterial Activity against *S. aureus*

ZOI data show that the antibacterial activity of cefazolin loaded PLL/$PLGA_{20}$ nanocoated SSDs increased with increasing amounts of cefazolin (Fig. 2). No antibacterial activity was observed on either the bare SSDs (control) or the PLL/$PLGA_{20}$ coated SSDs without cefazolin. The ZOI diameters increased from a mean of 17.2 ± 1.2 mm of PLL/$PLGA_{20}$ nanocoated samples at 76 μg/cm^2 cefazolin to 28.0 ± 0.9 mm of PLL/$PLGA_{20}$ nanocoated samples at 157 μg/cm^2 cefazolin.

The bacterial killing studies in Mueller Hinton (MH) broth show that, with increasing loading of cefazolin in the polypeptide nanofilms, the ability of the PLL/$PLGA_{20}$ nanofilms to inhibit the growth of *S. aureus* increased (Fig. 3). The PLL/$PLGA_{20}$ nanocoated SSDs with 76, 136, and 157 μg/cm^2 cefazolin kept inhibiting the growth of *S. aureus* at 37°C in MH broth for up to 12, 24, and 48 h, respectively. The PLL/$PLGA_{20}$ nanocoated SSDs without cefazolin, however, stimulated growth of *S. aureus* to some extent. Polypeptide nanocoatings with high cefazolin loading inhibited *S. aureus* growth for a long time (e.g. 7 days, see Supplementary Materials).

Influence of Polypeptide Nanofilms on *S. aureus* Adhesion

PLL/$PLGA_{20}$ nanofilms were found to substantially reduce *S. aureus* adhesion. A large quantity of *S. aureus* was adhered on the bare SSDs, while substantially fewer *S. aureus* was observed on PLL/$PLGA_{20}$ nanocoated SSDs (Fig. 4).

Influence of Cefazolin Loaded Polypeptide Nanofilms on Osteoblast Cell Adhesion

Osteoblast cells were cultured and seeded on SSD samples (Fig. 5A). At 2 h, significantly more osteoblast cells were attached to the PLL/$PLGA_{20}$ nanocoated surfaces than to bare SSDs, while dramatically fewer osteoblast cells were adhered to cefazolin loaded PLL/

$PLGA_{20}$ nanofilms compared to PLL/$PLGA_{20}$ nanofilms without cefazolin. The numbers of osteoblasts on bare SSDs and on cefazolin loaded PLL/$PLGA_{20}$ nanofilms were about the same. At 24 h, significantly more osteoblasts were observed on both the PLL/$PLGA_{20}$ nanocoated surfaces and the cefazolin loaded PLL/$PLGA_{20}$ nanocoated surfaces compared to the bare SSD samples, while no significant difference occurred between the PLL/$PLGA_{20}$ nanocoated samples and cefazolin loaded PLL/$PLGA_{20}$ nanocoated samples. This result was confirmed by examining the cells under confocal fluorescent microscopy. Fig. 5B shows that more osteoblast cells were adhered at 2 h on the PLL/$PLGA_{20}$ nanocoated SSDs compared to both bare SSDs and PLL/$PLGA_{20}$ nanocoated SSDs with cefazolin. At 24 h, the number of adhered osteoblasts on coated and coated with cefazolin SSDs are more than that adhered on non-coated SSDs.

Influence of Cefazolin Loaded Polypeptide Nanofilms on Osteoblast Cell Morphology

SEM observations show that, at 2 h incubation, the osteoblast cells that attached to PLL/$PLGA_{20}$ nanocoated SSDs and PLL/$PLGA_{20}$ nanocoated SSDs with cefazolin flattened and showed relatively smooth cell surfaces with a few long slender cell processes (Fig. 6). In contrast, cells on the bare SSDs were not spread out as much and were more round in shape. At 24 h incubation, osteoblasts on the three types of surfaces were all spread out and formed many long slender cell processes. Most cells were connected to their neighboring cells. The cells on PLL/$PLGA_{20}$ nanocoated SSDs still showed better spreading than those on bare SSDs.

Influence of Cefazolin Loaded Polypeptide Nanofilms on Osteoblast Cell Viability

MTT assay studies (Fig. 7) showed that the cell viability of osteoblasts adhered to PLL/$PLGA_{20}$ nanocoated SSDs, with and without cefazolin, was significantly higher than that of cells adhered to bare SSDs. No significant difference in cell viability was observed for the PLL/$PLGA_{20}$ nanocoated SSDs and PLL/$PLGA_{20}$ nanocoated SSDs with cefazolin.

Influence of Cefazolin Loaded Polypeptide Nanofilms on Osteoblast Cell Proliferation

The influence of PLL/$PLGA_{20}$ nanofilm and PLL/$PLGA_{20}$ nanofilm with cefazolin on osteoblast cell proliferation was studied at 1, 3, and 5 days (Fig. 8). No differences were observed at day 1. At days 3 and 5, the numbers of osteoblast cells grown on PLL/$PLGA_{20}$ nanocoated SSDs and PLL/$PLGA_{20}$ nanocoated SSDs with cefazolin were significantly higher than those on bare SSDs. The average cell numbers at 3 and 5 days on the PLL/$PLGA_{20}$ nanocoated SSDs with cefazolin was lower than those on the PLL/$PLGA_{20}$ nanocoated SSDs without cefazolin; however, the difference between these two types of samples was not statistically significant.

DISCUSSION

Bacteria are known to colonize on metal implants and form adherent bio-films[26]. Additionally, osteomyelitis is found to develop preferentially beneath the surfaces of fixation devices adjacent to bone[26,27]. Coating metal implants with a bactericidal film would inhibit bacteria from colonizing implant surfaces and provide a high antibiotic concentration in a local region commonly found as a nidus for bacterial infection. In this study, we developed polypeptide multilayer nanofilms as a biodegradable carrier for antibiotic delivery. Cefazolin, a widely used antibiotic in orthopedics, is negatively charged and was incorporated in PLL/$PLGA_{20}$ nanofilms based on electrostatic attraction[23]. The loading of cefazolin in PLL/$PLGA_{20}$ nanofilms on SSDs was controlled by cefazolin concentration (Fig. 1), and the tuning of cefazolin loading was translated to the tunability of *in vitro* antibacterial activity (Figs. 2 and 3).

Implant-associated infections are, at the cellular level, the result of bacterial adhesion onto biomaterial surfaces[11]. Upon implantation, a competition exists between the integration of the implant into surrounding tissue and the adhesion of bacteria to the implant surface[28]. A post-implantation "decisive period" (6 h), has been identified and is believed to be critical for preventing bacterial adhesion as well as achieving long-term success of implantation[29]. Implants are particularly susceptible to surface adhesion of bacteria within the decisive period, and once adhered, certain species of bacteria start to form a bio-film at the implant-tissue interface. The bio-films are remarkably resistant to both immune responses and systemic antibiotic therapies, and their formation is thought to be the primary cause of implant-associated infection. Therefore, inhibiting bacterial adhesion is often regarded as the most critical step in preventing implant-associated infection. In this study, polypeptide nanofilms were engineered on implant surfaces, enabling active release of antibacterial agents to reduce bacterial adhesion. The nanofilms were designed to release high fluxes of antibacterial agents during the post-implantation decisive period to effectively inhibit the initial adhesion of bacteria. More specifically, in the developed systems, a high percentage (84–93%) of loaded cefazolin was released within the first 2 h, and the cefazolin loaded PLL/$PLGA_{20}$ nanocoated samples were effective in inhibiting and killing bacteria for up to 12, 24, and 48 h or longer, depending on the amount of cefazolin loaded (Fig. 3). Moreover, PLL/$PLGA_{20}$ nanofilms (without cefazolin) could significantly inhibit *S. aureus* adhesion (Fig. 4) although the reasons for this are not clear. The negative charge of the outermost layer, i.e. PLGA, may play a role in inhibiting *S. aureus* adhesion and PLL may have some antibacterial activity[30]. Therefore, the developed cefazolin loaded polypeptide nanofilms may have the potential to prevent implant-associated infection.

Another advantage offered by polypeptide multilayer nanofilms is that their physicochemical properties[23] can be easily controlled thereby allowing better control of related cellular responses including cell adhesion, motility, spreading, growth, and differentiation. It has been shown that different parameters such as hydrophobicity and hydrophilicity[31], surface charge[32], roughness, surface free energy[33] and topography[34] affect cell adhesion. In the present study, we tested the cellular responses of osteoblasts to cefazolin loaded polypeptide multilayer nanofilms. Cell culture studies at 2 and 24 h showed that polypeptide multilayer nanofilms (without cefazolin) improved the adhesion of osteoblasts dramatically. The incorporation of cefazolin in polypeptide multilayer nanofilms decreased the adhesion of osteoblasts at 2 h culturing; this effect vanished at 24 h, which was probably due to the substantial release of cefazolin within the first few hours. As a result, no difference in osteoblast cell adhesion was observed at 24 h between PLL/$PLGA_{20}$ nanocoated samples and PLL/$PLGA_{20}$ nanocoated samples with cefazolin; cefazolin loaded polypeptide nanofilms have similar (2 h) or enhanced (24 h) osteoblast cell adhesion compared to the control (Fig. 5A). Our results also showed that PLL/$PLGA_{20}$ nanofilms, with and without cefazolin, could improve the viability and proliferation of osteoblasts, and no differences at a relatively long time period (a few days) were found in viability and proliferation of osteoblasts between the PLL/$PLGA_{20}$ nanofilms and PLL/$PLGA_{20}$ nanofilms with cefazolin (Figs. 7 and 8). These results suggested, for the first time, that the developed antibiotic loaded polypeptide multilayer nanofilms, used as surface coatings, are biocompatible with osteoblasts and promote osteoblast proliferation.

In summary, this study showed that a biodegradable implant nanofilms can be engineered to have antibacterial activity against organisms frequently associated with osteomyelitis. Polypeptide multilayer nanofilms, with or without cefazolin, were found to be biocompatible with osteoblasts. The developed polypeptide nanocoated implants could be used prophylactically to reduce the incidence of soft tissue and bone infection that frequently complicate open fractures. Meanwhile, the nanocoatings may improve bone healing through

improving osteoblast cell adhesion, viability, and proliferation. In the future, the effects of cefazolin loaded polypeptide nanofilms on osseointegration will be studied.

Supplementary Material

Refer to Web version on PubMed Central for supplementary material.

Acknowledgments

The authors acknowledge financial support from the AO Foundation, NSF (Grant Number OISE-0737735), NASA WV EPSCoR, and WVU. Project S-07-43L was supported by the AO Research Fund of the AO Foundation. The authors appreciate the use of confocal laser scanning microscope at the Microscopic Imaging Facilities at West Virginia University Health Sciences Center. We acknowledge John G. Thomas, PhD (Department of Pathology) for the contribution of *S. aureus* and consultation on bacterial culture. We thank Karen Martin for assisting in confocal imaging, Suzanne Smith for proofreading, Nina Clovis for laboratory training, and Vincent Kish for assistance in SEM sample preparation. MH also thanks the E.J. Van Liere fellowship.

REFERENCES

1. Darouiche RO. Treatment of infections associated with surgical implants. N Engl J Med. 2004; 350(14):1422–1429. [PubMed: 15070792]
2. Sanderson PJ. Preventing infection in orthopaedic implants. J Antimicrob Chemother. 1989; 24(3): 277–280. [PubMed: 2681114]
3. Taylor GJ, Bannister GC, Calder S. Perioperative wound infection in elective orthopaedic surgery. J Hosp Infect. 1990; 16(3):241–247. [PubMed: 1979574]
4. Anderson JM. Biological responses to materials. Ann Rev Mater Res. 2001; 31:81–110.
5. An YH, Friedman RJ. Prevention of sepsis in total joint arthroplasty. J Hosp Infect. 1996; 33(2):93–108. [PubMed: 8808743]
6. Calhoun JH, Manring MM. Adult osteomyelitis. Infect Dis Clin North Am. 2005; 19(4):765–786. [PubMed: 16297731]
7. Barton AJ, Sagers RD, Pitt WG. Bacterial adhesion to orthopedic implant polymers. J Biomed Mater Res. 1996; 30(3):403–410. [PubMed: 8698704]
8. Gotz F. Staphylococcus and biofilms. Mol Microbiol. 2002; 43(6):1367–1378. [PubMed: 11952892]
9. Gristina AG. Implant failure and the immuno-incompetent fibro-inflammatory zone. Clin Orthop Relat Res. 1994; 298:106–118. [PubMed: 8118964]
10. Khardori N, Yassien M. Biofilms in device-related infections. J Ind Microbiol. 1995; 15(3):141–147. [PubMed: 8519469]
11. Hetrick EM, Schoenfisch MH. Reducing implant-related infections: active release strategies. Chem Soc Rev. 2006; 35(9):780–789. [PubMed: 16936926]
12. Price JS, Tencer AF, Arm DM, Bohach GA. Controlled release of antibiotics from coated orthopedic implants. J Biomed Mater Res. 1996; 30(3):281–286. [PubMed: 8698690]
13. Lucke M, Schmidmaier G, Sadoni S, et al. Gentamicin coating of metallic implants reduces implant-related osteomyelitis in rats. Bone. 2003; 32(5):521–531. [PubMed: 12753868]
14. Stigter M, Bezemer J, de Groot K, et al. Incorporation of different antibiotics into carbonated hydroxyapatite coatings on titanium implants, release and antibiotic efficacy. J Control Release. 2004; 99(1):127–137. [PubMed: 15342186]
15. Humphrey JS, Mehta S, Seaber AV, et al. Pharmacokinetics of a degradable drug delivery system in bone. Clin Orthop Relat Res. 1998; 349:218–224. [PubMed: 9584386]
16. Nablo BJ, Schoenfisch MH. Poly(vinyl chloride)-coated sol-gels for studying the effects of nitric oxide release on bacterial adhesion. Biomacromolecules. 2004; 5(5):2034–2041. [PubMed: 15360321]
17. Decher G. Fuzzy nanoassemblies: Toward layered polymeric multicomposites. Science. 1997; 277(5330):1232–1237.

18. Lvov Y, Ariga K, Ichinose I, et al. Assembly of multicomponent protein films by means of electrostatic layer-by-layer adsorption. J Am Chem Soc. 1995; 117(22):6117–6123.
19. Kong W, Wang LP, Gao ML, et al. Immobilized Bilayer Glucose-Isomerase in Porous Trimethylamine Polystyrene-Based on Molecular Deposition. Chem Commun. 1994; 1994(11): 1297–1298.
20. Ladam G, Schaaf P, Cuisinier FJG, et al. Protein adsorption onto auto-assembled polyelectrolyte films. Langmuir. 2001; 17:878–882.
21. Ladam G, Schaad P, Voegel JC, et al. In situ determination of the structural properties of initially deposited polyelectrolyte multilayers. Langmuir. 2000; 16:1249–1255.
22. Li B, Jiang B, Boyce B, Lindsey B. Multilayer polypeptide nanoscale coatings for the prevention of biomedical device associated infections. Biomaterials. 2009; 30:2552–2558. [PubMed: 19215980]
23. Jiang B, Li B. Polypeptide nanocoatings for preventing dental and orthopaedic device-associated infection: pH-induced antibiotic capture, release, and antibiotic efficacy. J Biomed Mater Res B. 2009; 88(2):332–338.
24. Jiang B, Li B. Tunable drug loading and release from polypeptide multilayer nanofilms. Int J Nanomedicine. 2009; 4(1):37–53. [PubMed: 19421369]
25. Helmerhorst EJ, Van't Hof W, Veerman EC, et al. Synthetic histatin analogues with broad-spectrum antimicrobial activity. Biochem J. 1997; 326(Pt 1):39–45. [PubMed: 9337848]
26. Webb LX, Holman J, de Araujo B, et al. Antibiotic resistance in staphylococci adherent to cortical bone. J Orthop Trauma. 1994; 8:28–33. [PubMed: 8169691]
27. Chang CC, Merritt K. Infection at the site of implanted materials with and without preadhered bacteria. J Orthop Res. 1994; 12(4):526–531. [PubMed: 8064483]
28. Gristina AG. Biomaterial-centered infection: microbial adhesion versus tissue integration. Science. 1987; 237(4822):1588–1595. [PubMed: 3629258]
29. Poelstra KA, Barekzi NA, Rediske AM, et al. Prophylactic treatment of gram-positive and gram-negative abdominal implant infections using locally delivered polyclonal antibodies. J Biomed Mater Res. 2002; 60:206–215. [PubMed: 11835177]
30. Nishikawa M, Ogawa K. Inhibition of epsilon-poly-L-lysine biosynthesis in Streptomycetaceae bacteria by short-chain polyols. Appl Environ Microbiol. 2006; 72:2306–2312. [PubMed: 16597924]
31. Grinnell F, Feld MK. Fibronectin adsorption on hydrophilic and hydrophobic surfaces detected by antibody binding and analyzed during cell adhesion in serum-containing medium. J Biol Chem. 1982; 257(9):4888–4893. [PubMed: 7068668]
32. Qiu Q, Sayer M, Kawaja M, et al. Attachment, morphology, and protein expression of rat marrow stromal cells cultured on charged substrate surfaces. J Biomed Mater Res. 1998; 42:117–127. [PubMed: 9740014]
33. Kapur R, Rudolph AS. Cellular and cytoskeleton morphology and strength of adhesion of cells on self-assembled monolayers of organosilanes. Exp Cell Res. 1998; 244(1):275–285. [PubMed: 9770370]
34. Curtis AS, Varde M. Control of cell behavior: Topological factors. J Natl Cancer Inst. 1964; 33:15–26. [PubMed: 14202300]

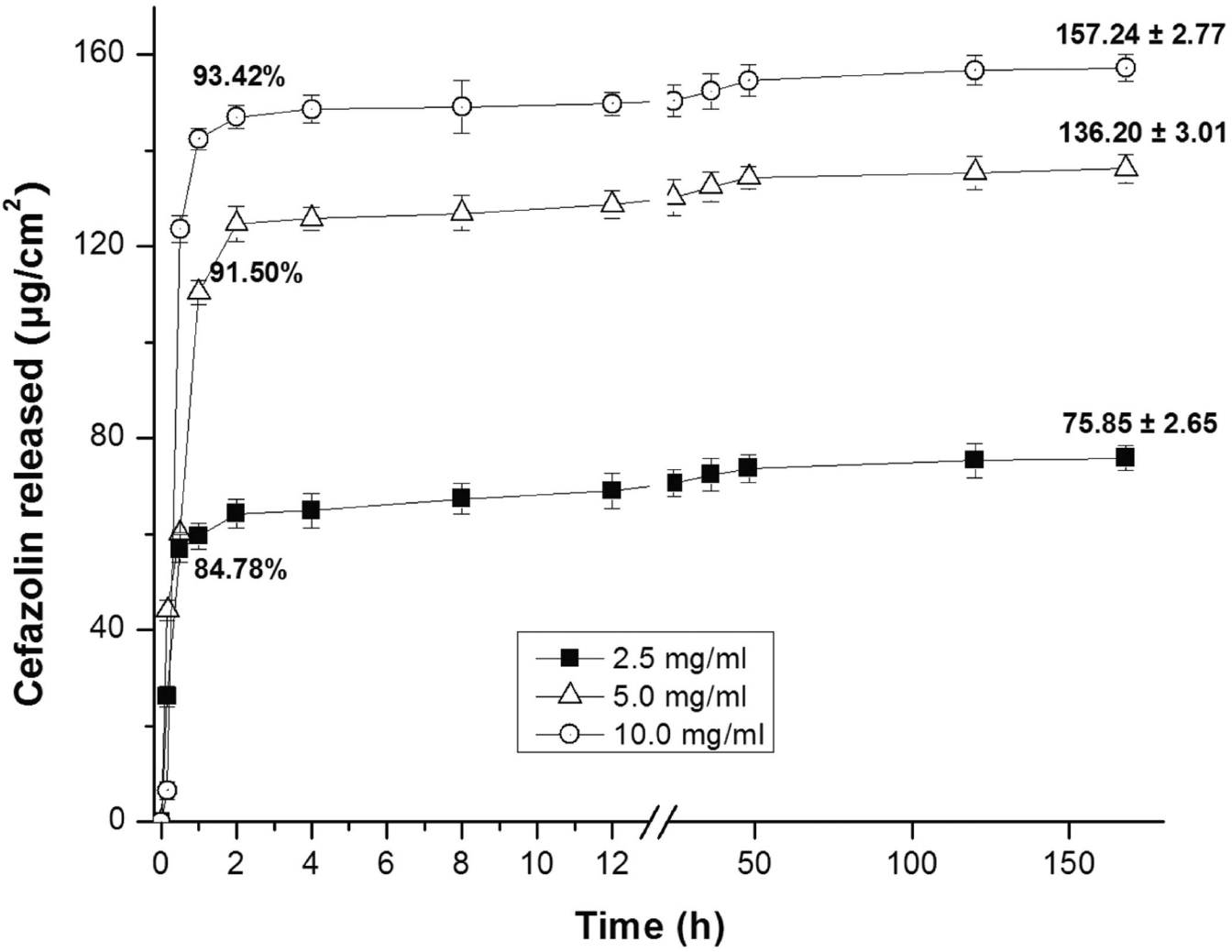

Figure 1.
Release profiles of PLL/PLGA$_{20}$ nanocoated SSDs loaded with cefazolin at three different concentrations. Three samples were tested at each cefazolin concentration.

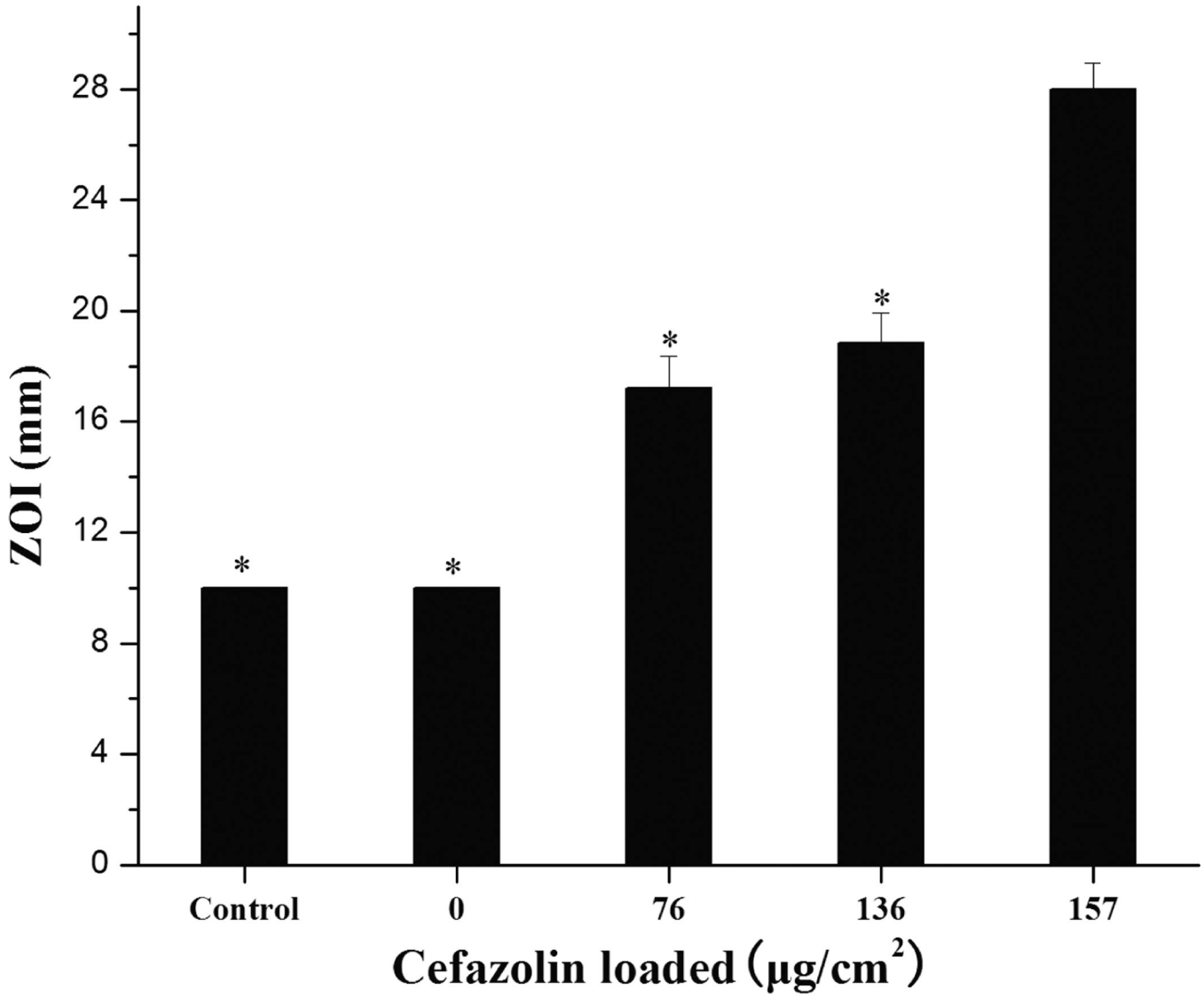

Figure 2.

ZOI data *vs.* amount of cefazolin loaded in PLL/$PLGA_{20}$ nanofilms. Bare SSDs were used as a control. The diameter of SSDs was 10 mm. *$p<0.05$ compared with 157 μg/cm^2 group.

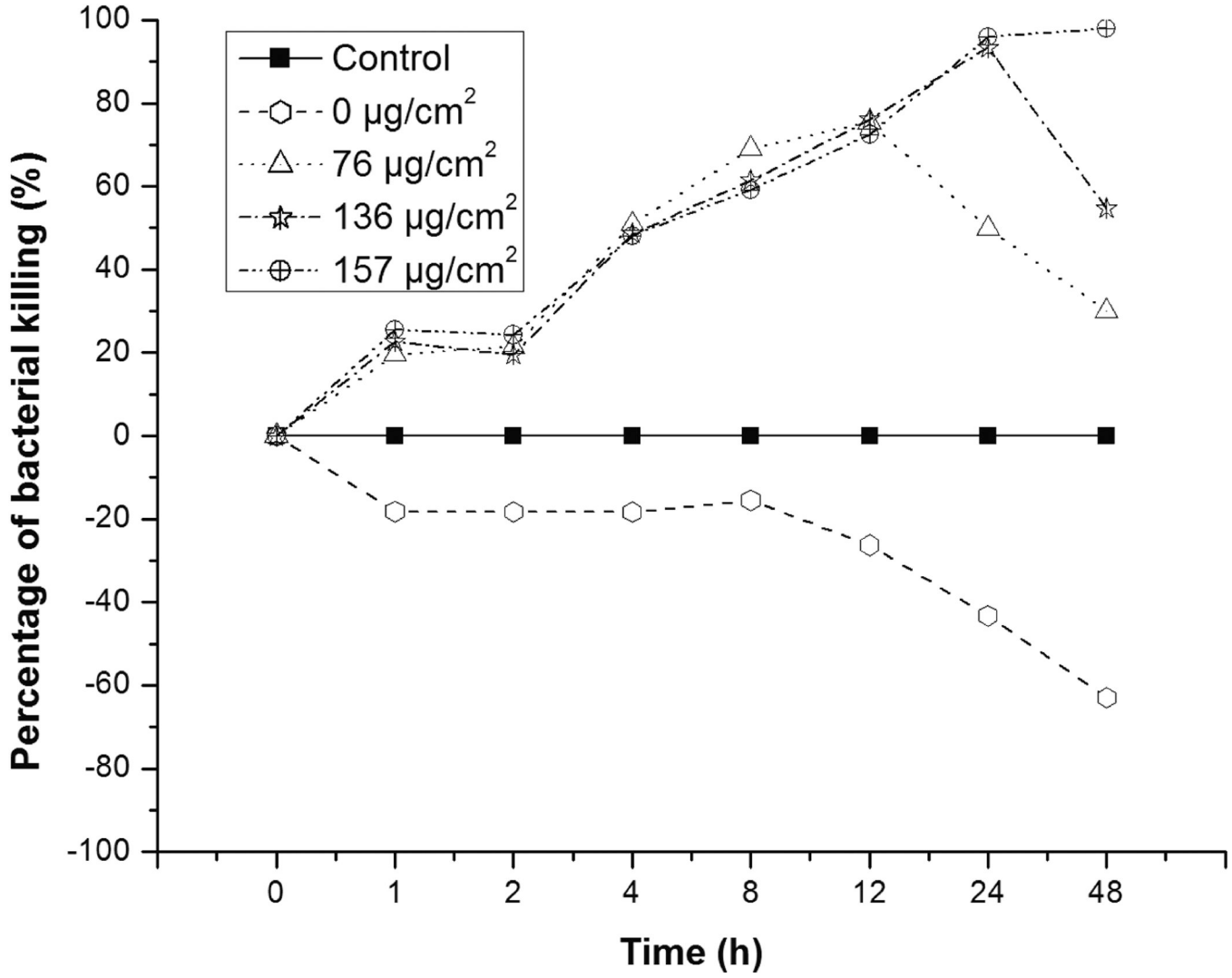

Figure 3.
Percentage of *S. aureus* killed in MH broth based on OD measurements. 1×10^7 CFU/ml of *S. aureus* was used. Percentage of killing = {1 − [(OD of sample − OD of MH broth)/(OD of control − OD of MH broth)]} × 100%.

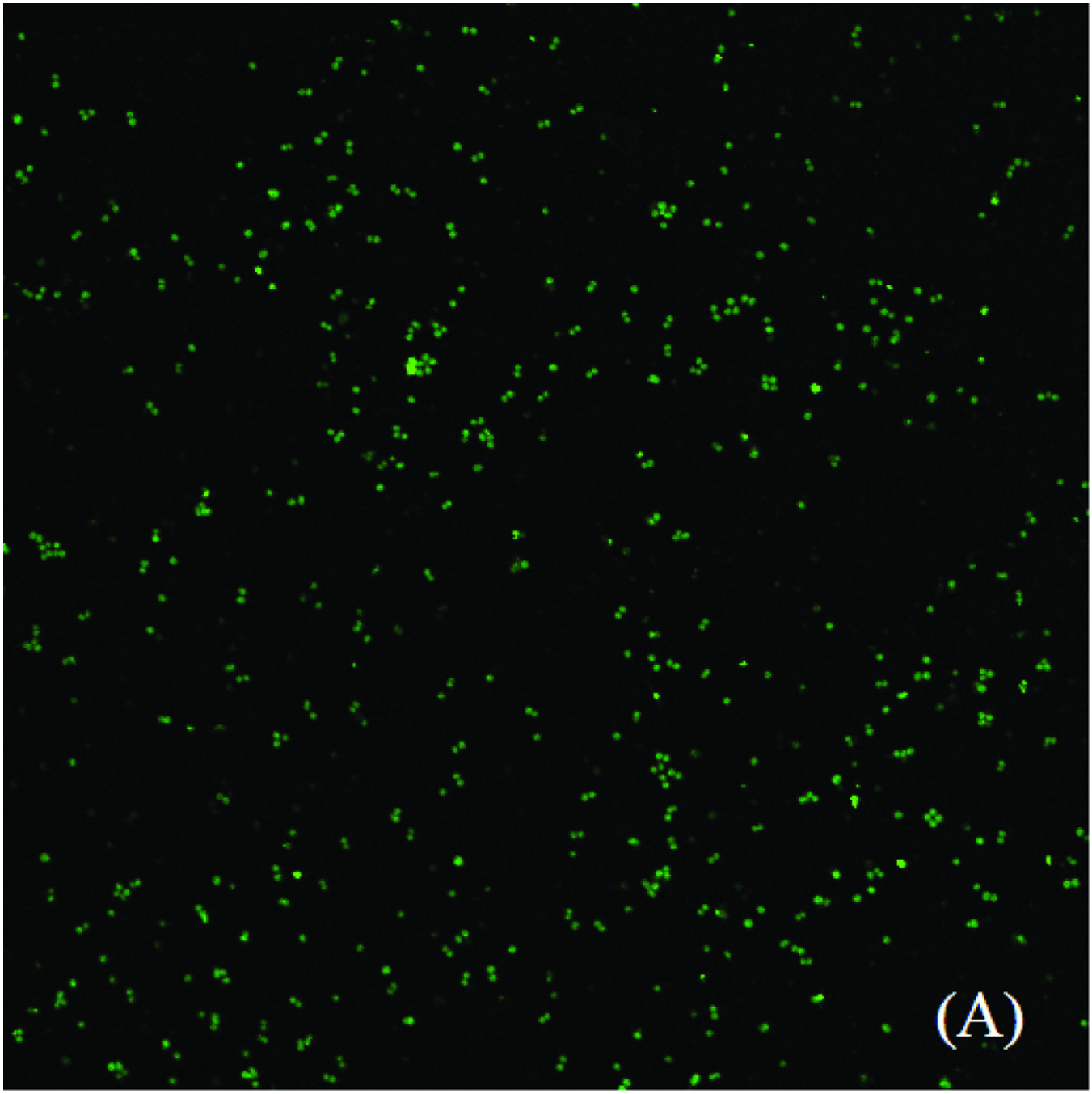

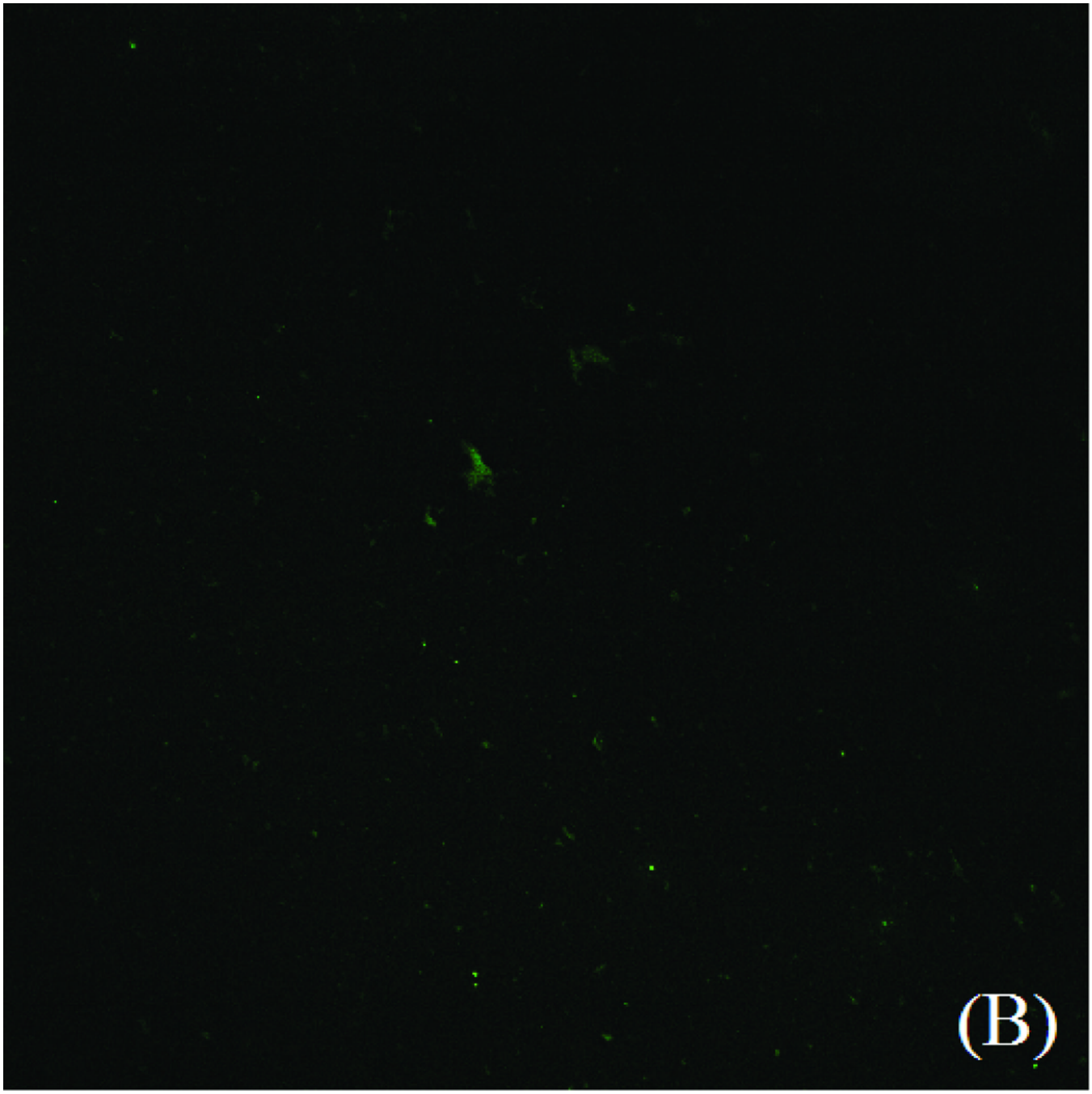

Figure 4.
S. aureus adhesion on (A) bare SSDs and (B) PLL/$PLGA_{20}$ nanocoated SSDs (without cefazolin) after 2 h incubation.

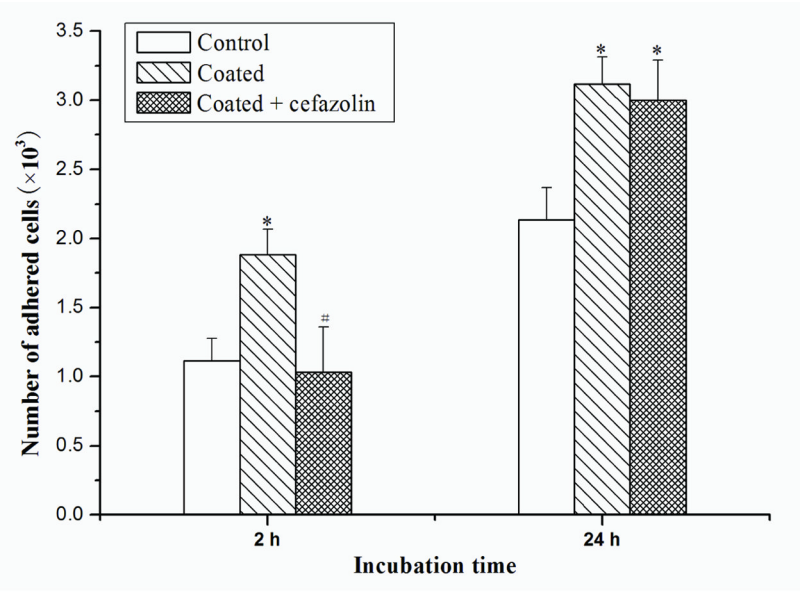

A.

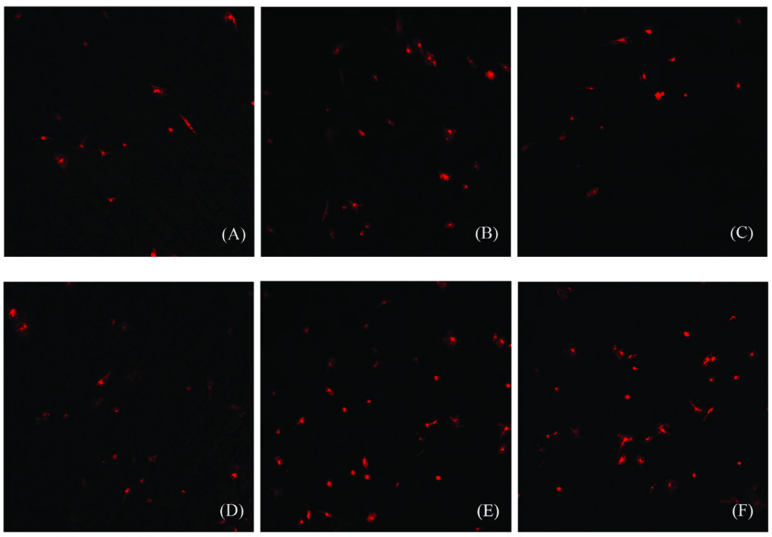

B.

Figure 5.

A. Influences of PLL/PLGA$_{20}$ nanofilms and cefazolin (157 μg/cm^2) loaded PLL/PLGA$_{20}$ nanofilms on osteoblast cell adhesion. *$p<0.05$ compared to non-coated group; $^{\#}p<0.05$ compared to coated group.

B. Fluorescence labeling of adhered osteoblasts on bare SSDs (A and D), PLL/PLGA$_{20}$ nanocoated SSDs (B and E), and PLL/PLGA$_{20}$ nanocoated SSDs with 157 μg/cm^2 cefazolin (C and F) after 2 (A, B, and C) and 24 h (D, E, and F) cell seeding.

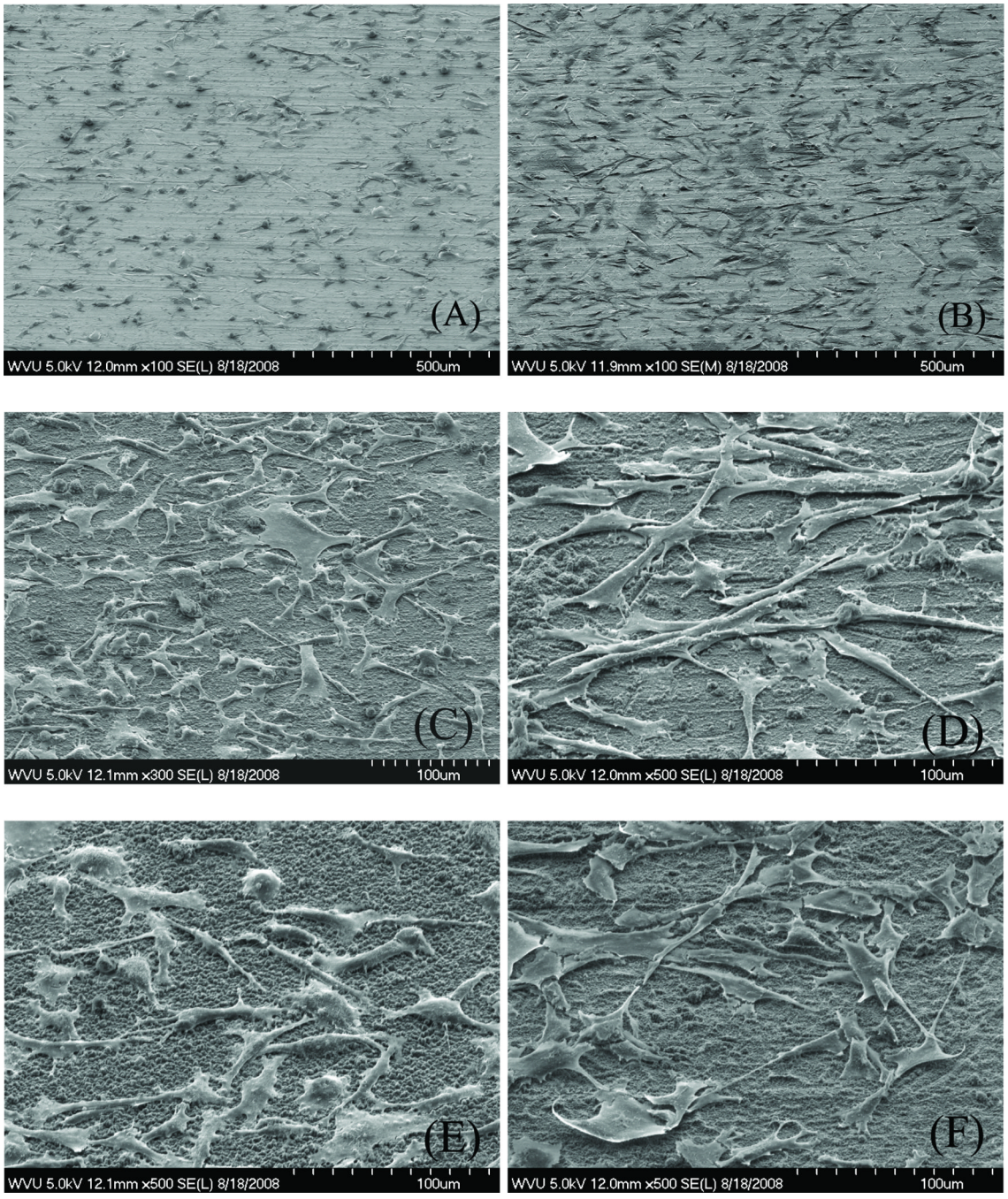

Figure 6.

SEM images of osteoblasts adhered to bare SSDs (A and B), PLL/$PLGA_{20}$ nanocoated SSDs (C and D), and PLL/$PLGA_{20}$ nanocoated SSDs with 157 μg/cm^2 cefazolin (E and F) at 2 (A, C, and E) and 24 h (B, D, and F) culturing.

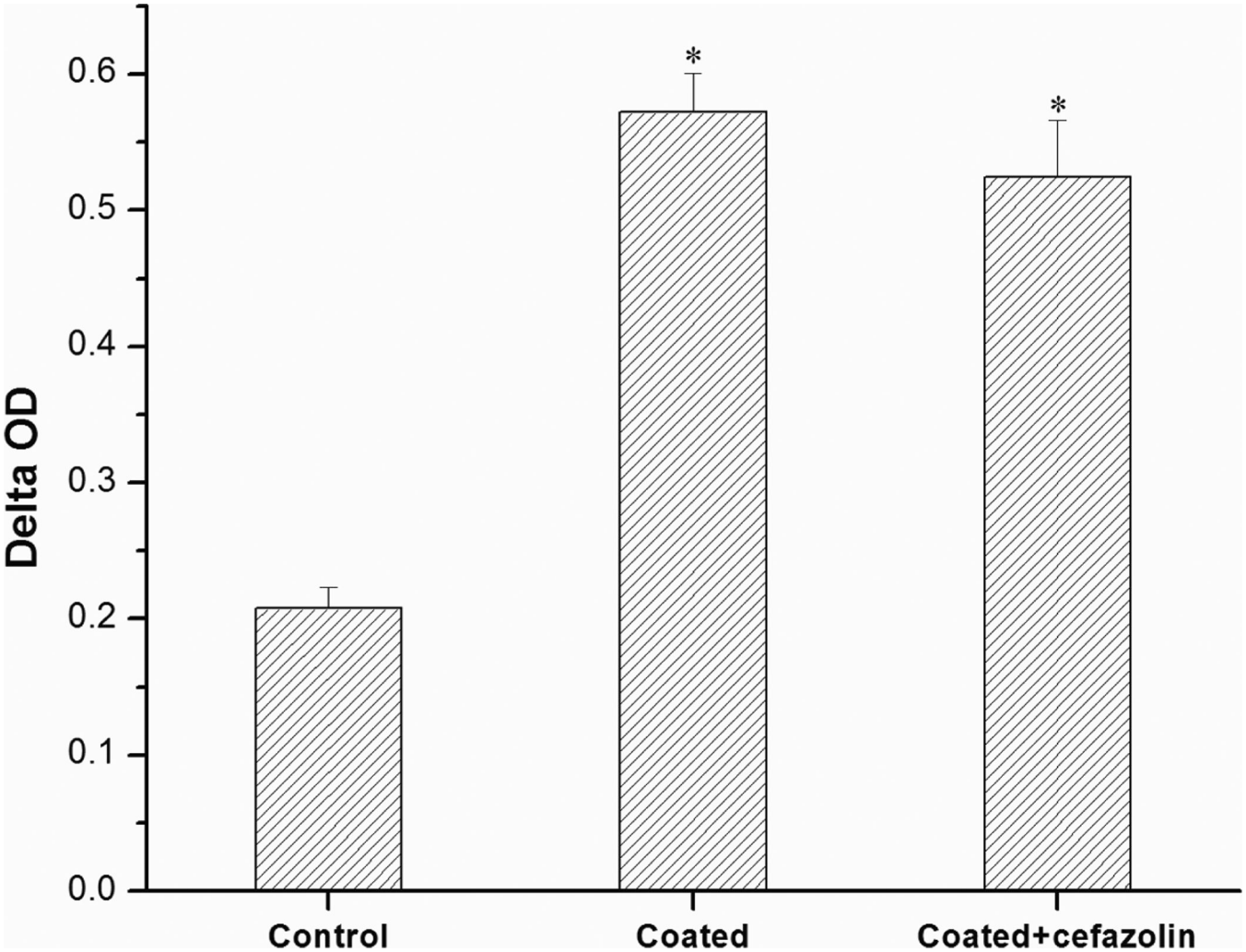

Figure 7.
Influences of PLL/$PLGA_{20}$ nanofilms and cefazolin (157 μg/cm^2) loaded PLL/$PLGA_{20}$ nanofilms on osteoblast viability. *$p<0.05$ compared to bare SSD samples.

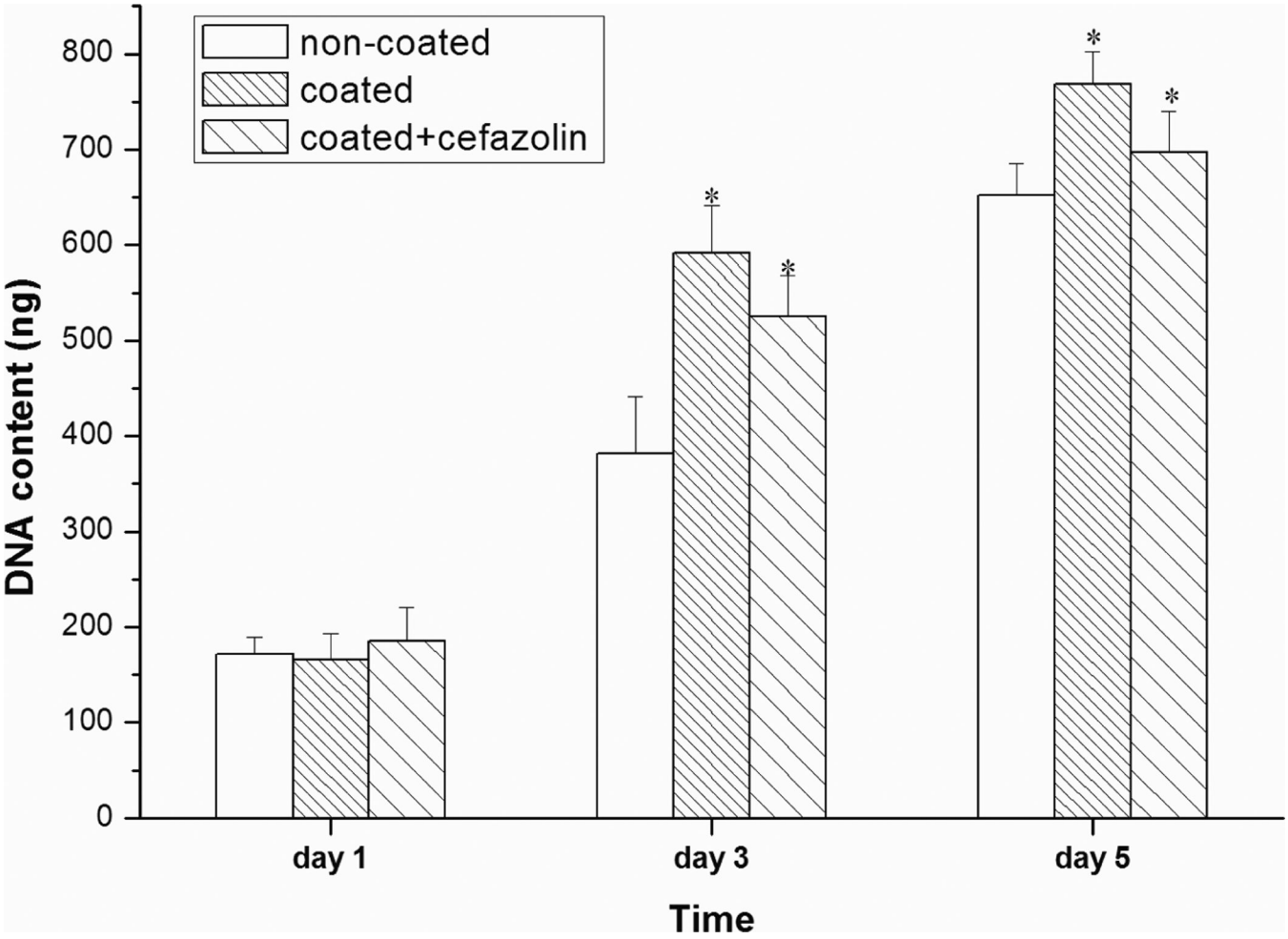

Figure 8.
Influences of PLL/PLGA$_{20}$ nanofilms and cefazolin (157 μg/cm^2) loaded PLL/PLGA$_{20}$ nanofilms on osteoblast proliferation. *$p<0.05$ compared to bare SSD samples.